Relativistic descriptions of final-state interactions in neutral-current neutrino-nucleus scattering at MiniBooNE kinematics

Andrea Meucci, Carlotta Giusti, and Franco Davide Pacati

Dipartimento di Fisica Nucleare e Teorica, Università degli Studi di Pavia,
and INFN, Sezione di Pavia, via A. Bassi 6, I-27100 Pavia, Italy

(Received 18 October 2011; published 8 December 2011)

The analysis of the recent neutral-current neutrino-nucleus scattering cross sections measured by the MiniBooNE Collaboration requires relativistic theoretical descriptions also accounting for the role of final-state interactions. In this work, we evaluate differential cross sections with the relativistic distorted-wave impulse approximation and with the relativistic Green's function model to investigate the sensitivity to final-state interactions. The role of the strange-quark content of the nucleon form factors is also discussed.

DOI: 10.1103/PhysRevD.84.113003 PACS numbers: 25.30.Pt, 12.15.Mm, 13.15.+g, 24.10.Jv

I. INTRODUCTION

The MiniBooNE Collaboration has recently reported [1] a measurement of the flux-averaged differential cross section as a function of the four-momentum transferred squared, $Q^2 = -q^\mu q_\mu$, for neutral-current elastic (NCE) neutrino scattering on CH_2 in a Q^2 range up to $\approx 1.65\ (\mathrm{GeV}/c)^2$. The neutrino-nucleus NCE reaction in MiniBooNE may be considered as scattering of an incident neutrino with a single nucleon bound in carbon or free in hydrogen, but it can also be sensitive to contributions from collective nuclear effects, whose clear understanding is crucial for the analysis of ongoing and future neutrino oscillation measurements [1–6]. In addition, NCE processes can be used to look for strange-quark contributions in the nucleon that may show up through the isoscalar weak current.

Recent results on parity-violating electron scattering at $Q^2 = 0.1\ (\mathrm{GeV}/c)^2$ [7] indicate that the strangeness contribution to the electric charge and magnetic moment of the nucleon is consistent with zero at 95% confidence level. In the axial form factor, under the usual assumption of a dipole Q^2 dependence, the only free parameters within the relativistic Fermi gas (RFG) model [8,9] are the nucleon axial mass M_A and the strange-quark contribution Δs, determining the value of the axial form factor at $Q^2 = 0$, which is related to the fraction of the nucleon spin carried by the strange quark. Recent charged-current quasielastic (CCQE) neutrino-nucleus measurements [2,10] reported values of $M_A \approx 1.2$–$1.3\ \mathrm{GeV}/c^2$, significantly larger than the world average value from the deuterium data of $M_A = 1.03\ \mathrm{GeV}/c^2$ [11,12]. In agreement with these new results, the MiniBooNE NCE data provide a best fit for $M_A = 1.39 \pm 0.11\ \mathrm{GeV}/c^2$.

A measurement of $\nu(\bar{\nu})$-proton elastic scattering at the Brookhaven National Laboratory [13] at low Q^2 suggested a nonzero value for the strange axial-vector form factor. However, the Brookhaven National Laboratory data cannot provide us decisive conclusions when also strange vector form factors are taken into account [14]. A determination of the strange form factors through a simultaneous analysis of νp, $\bar{\nu} p$, and $\vec{e} p$ elastic scattering is performed in Ref. [15].

Since cross section measurements are a very hard experimental task, ratios of cross sections have been proposed as alternative ways to search for strangeness [16,17]. Moreover, they are expected to be less sensitive to distortion effects [18,19]. Taking advantage of the fact that at $Q^2 \geq 0.7\ (\mathrm{GeV}/c)^2$ single proton events can be satisfactorily separated from neutron and multiple nucleon events, the MiniBooNE Collaboration used the ratio of proton-to-nucleon cross sections to extract the strangeness contribution to the axial form factor [1]. The resulting value is $\Delta s = 0.08 \pm 0.26$. Although affected by large systematic errors because of difficulties in the proton/neutron identification, this result is anyhow very interesting, since this is the first attempt to measure Δs using this ratio. In addition, exploiting its data sample of neutrino-nucleus events, the MiniBooNE Collaboration has also focused on the neutral-to-charged-current ratio [1,2], which can provide us with useful and complementary information.

The energy region considered in the MiniBooNE experiments, with neutrino energy up to ≈ 3 GeV and average energy of ≈ 0.8 GeV, requires the use of a relativistic model, where not only relativistic kinematics should be considered, but also nuclear dynamics and current operators should be described within a relativistic framework. From the comparison with electron scattering data, the RFG turns out to be a too naive model to correctly account for the nuclear dynamics, and thus the larger axial mass needed by the RFG could be considered as an effective value to incorporate nuclear effects into the calculation. Regardless of this question, a comparison between the results of different models and the NCE MiniBooNE data is important to clarify the role of the various ingredients entering the description of the reaction.

At intermediate energy, quasielastic (QE) electron scattering calculations [20,21], which were able to successfully

 © 2011 American Physical Society

describe a wide number of experimental data, can provide a useful tool to study neutrino-induced processes. However, a careful analysis of ν-nucleus NCE reactions introduces additional complications, as the final neutrino cannot be measured in practice and a final hadron has to be detected: the corresponding cross sections are therefore semi-inclusive in the hadronic sector and inclusive in the leptonic one. Several sophisticated models have been applied in recent years to ν-nucleus scattering reactions and some of them have been compared with the MiniBooNE data, both in the CCQE and in the NCE channels. At the level of the impulse approximation (IA), models based on the use of a realistic spectral function [22,23], which are built within a nonrelativistic framework, underestimate the experimental CCQE and NCE cross sections unless M_A is enlarged with respect to the world average value. The same results are obtained by models based on the relativistic IA [24–26]. However, the reaction may have significant contributions from effects beyond the IA in some kinematic regions where the neutrino flux for the experiment has significant strength. For instance, in the models of Refs. [27–31], the contribution of multinucleon excitations to CCQE scattering has been found sizable and able to bring the theory in agreement with the experimental MiniBooNE cross sections without increasing the value of M_A. Fully relativistic microscopic calculations of two-particle-two-hole (2p-2h) contributions are very involved and may be bound to model dependent assumptions. The part of the 2p-2h excitations which may be reached through two-body meson-exchange currents—in particular, the contribution of the vector meson-exchange currents in the 2p-2h sector, evaluated in the model of Ref. [32]—has been incorporated in a phenomenological approach based on the superscaling behavior of electron scattering data [33,34].

Within the QE kinematic domain, the treatment of the final-state interactions (FSI) between the ejected nucleon and the residual nucleus is an essential ingredient for the comparison with data. The relevance of FSI has been clearly stated in the case of exclusive $(e, e'N)$ processes, where the use of complex optical potentials in the distorted-wave impulse-approximation (DWIA) is required [20,21,35–41]. In the exclusive reaction, where the final state is completely determined, the absorptive imaginary part of the optical potential accounts for the flux lost to different final nuclear states. In contrast, the analysis of inclusive reactions needs all final-state channels to be retained, *i.e.*, the flux must be conserved and the DWIA based on the use of an absorptive complex potential should be dismissed. Different approaches have been used to describe FSI in relativistic calculations for the inclusive QE electron- and neutrino-nucleus scattering [42–48]. Besides the relativistic plane-wave impulse approximation (RPWIA), where FSI are simply neglected, FSI have been included in DWIA calculations where the final nucleon state is evaluated with purely real potentials, either retaining only the real part of the relativistic energy-dependent optical potential (rROP), or using the same relativistic mean field (RMF) potential considered in describing the initial nucleon state . Although conserving the flux, the rROP is unsatisfactory from a theoretical point of view, since it relies on an energy-dependent potential, which reflects the different contribution of open inelastic channels for each energy, and under such conditions, dispersion relations dictate that the potential should have a nonzero imaginary term [49]. On the other hand, in the RMF model, the same strong energy-independent real potential is used for both bound and scattering states. It fulfills the dispersion relations [49] and also the continuity equation.

In a different description of FSI, relativistic Green's function (RGF) techniques [45–48,50,51] are used. This formalism allows us to reconstruct the flux lost into nonelastic channels in the case of the inclusive response starting from the complex optical potential which describes elastic nucleon-nucleus scattering data. Thus, it provides a consistent treatment of FSI in the exclusive and in the inclusive scattering and gives a good description of (e, e') data [46,47]. Moreover, due to the analiticity properties of the optical potential, the RGF model fulfills the Coulomb sum rule [46,49,50].

These different descriptions of FSI have been compared in Ref. [47] for the inclusive QE electron scattering, in Ref. [48] for the CCQE neutrino scattering, and in Ref. [52] with the CCQE MiniBooNE data, which are reasonably described by the RGF results without the need to increase the value of M_A and are generally underestimated by the other models.

In this paper, different relativistic descriptions of FSI for neutral-current (NC) ν-nucleus reactions in the quasielastic region are presented and compared with the NCE MiniBooNE data. In these reactions, a final nucleon is detected, like in the exclusive scattering, but since the final lepton cannot be detected, the final nuclear state is not completely determined and the cross section includes many possible final-state channels. In Refs. [18,19,53–55], such a semi-inclusive scattering was treated with the same relativistic DWIA (relativistic distorted-wave impulse approximation [RDWIA]) model which was successfully applied to the exclusive $(e, e'N)$ reaction, as a process where the cross section is obtained from the sum of all the integrated exclusive one-nucleon knockout channels. Results for both the semi-inclusive charged-current and NC cross sections were presented and the effects of possible strange-quark contributions on the cross sections and on other observables were discussed. In RDWIA calculations, the imaginary part of the optical potential produces a loss of flux that accounts for the flux lost in each considered channel towards other final channels. Some of these reaction channels are not included in the experimental cross section when an emitted nucleon is detected and for these channels this treatment of FSI is correct. There are, however, other channels, which are excluded by the RDWIA approach but which can contribute to the semi-inclusive reaction. Some of these contributions may be small or negligible for the specific final state considered in the exclusive reaction, but may be much more important for all the final states of the semi-inclusive reaction. The flux lost towards these channels can be recovered in the RGF, where the imaginary part of the optical potential redistributes the strength in all the channels and the total flux is conserved. The RGF, however, describes the inclusive process and, as such, can include also contributions of channels which are not included in the cross sections of the semi-inclusive reactions. Thus, according to the approach adopted to describe FSI, the RDWIA can produce cross sections smaller and the RGF larger than the experimental ones. The relevance of the contributions neglected in the RDWIA and added in the RGF depends on kinematics. It is not easy to disentangle the role of each specific contribution, in particular, if we consider that both RDWIA and RGF calculations make use of phenomenological optical potentials, obtained through a fit of elastic proton-nucleus scattering data.

In spite of these uncertainties, the comparison between the results of the RDWIA and RGF models with the MiniBooNE data can be helpful for a deeper understanding of the role of FSI in the analysis of NCE data.

II. RESULTS AND DISCUSSION

In all the calculations presented in this work, the bound nucleon states are taken as self-consistent Dirac-Hartree solutions derived within a relativistic mean field approach using a Lagrangian containing σ, ω, and ρ mesons [56–58]. The energy-dependent but A-independent (EDAI [the A represents the atomic number]) parameterization for the complex phenomenological potential of Refs. [59,60], which is fitted to elastic proton-^{12}C scattering data, has been used. The energy-dependent and A-dependent (EDAD1) parameterization, which is fitted to elastic proton scattering data on several nuclei in an energy range up to 1040 MeV, has also been used for some calculations. We note that whereas EDAD1 is a global parameterization, EDAI is a single-nucleus parameterization, which is constructed to better reproduce the elastic proton-^{12}C phenomenology [60], and also leads to CCQE results in better agreement with the MiniBooNE data [52].

In Fig. 1, the NCE ($\nu N \rightarrow \nu N$) cross sections averaged over the neutrino flux are shown as a function of Q^2 and compared with the MiniBooNE data [1]. Calculations are performed in the RPWIA and RDWIA with $M_A = 1.03$ and $1.39\ \mathrm{GeV}/c^2$ and neglect possible strange-quark effects. A larger value of M_A gives a larger cross section, because of the dominant role played by the axial-vector current in NC scattering, but the enhancement is not linearly proportional

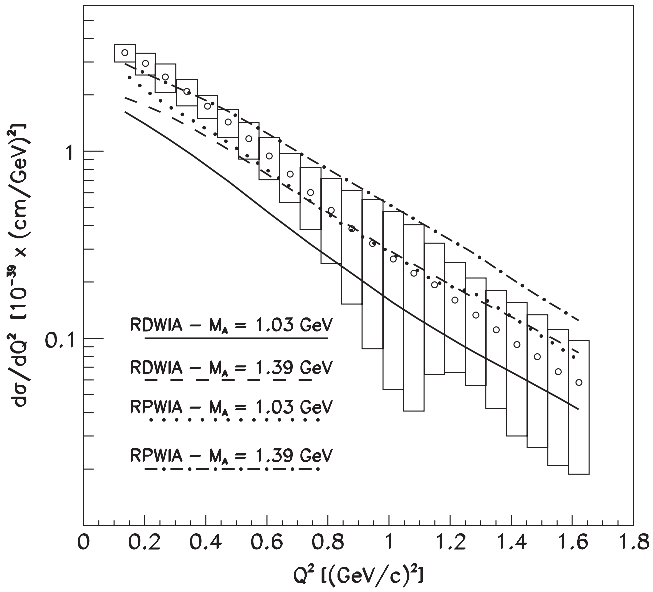

FIG. 1. NCE flux-averaged ($\nu N \rightarrow \nu N$) cross section as a function of Q^2, calculated with two different values of the axial mass in the RDWIA (solid and dashed lines) and RPWIA (dotted and dotted-dashed lines). The data are from MiniBooNE [1].

to M_A and, therefore, also the shape of the cross section is slightly modified. In the comparison with data, the RPWIA results show a generally satisfactory—although not perfect—agreement with the magnitude, while some differences are obtained with respect to the shape of the experimental cross section. In the RPWIA, however, FSI are completely neglected. The RDWIA results are smaller than the RPWIA ones and therefore also smaller than the experimental data. This is due to the imaginary part of the optical potential, which in the RDWIA gives an absorption that reduces the calculated cross section and neglects the contributions of some channels that can be included in the measured cross section. In Fig. 1, the RDWIA calculations with the EDAI potential generally underestimate the NCE cross section, unless $Q^2 \geq 0.8\ (\mathrm{GeV}/c)^2$ for $M_A = 1.03\ \mathrm{GeV}/c^2$ and $Q^2 \geq 0.6\ (\mathrm{GeV}/c)^2$ for $M_A = 1.39\ \mathrm{GeV}/c^2$. These results are essentially related to the role of the imaginary part of the optical potential and, in particular, for the kinematics at low Q^2 where the NCE data are underestimated. However, we have already noticed that the RDWIA neglects the contributions of some channels that can be included in the measured NCE cross section. We have checked that close RDWIA results are obtained with the EDAD1 potential, but for small values of Q^2, where there are visible differences that can be attributed to the different imaginary parts of the two optical potentials in the low-energy region.

In Fig. 2, we show our RDWIA results with $\Delta s = -0.18$ and $+0.34$ and $M_A = 1.39\ \mathrm{GeV}/c^2$. These are the upper and lower limits for Δs found by MiniBooNE [1]. The results for $\Delta s = 0$ with $M_A = 1.03$ and $1.39\ \mathrm{GeV}/c^2$ are

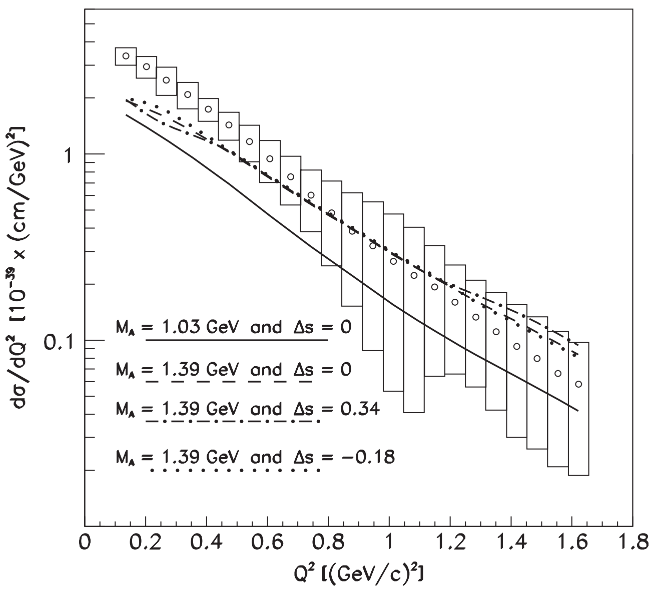

FIG. 2. NCE flux-averaged ($\nu N \rightarrow \nu N$) cross section as a function of Q^2, calculated in the RDWIA with three different values of Δs and $M_A = 1.39\ \mathrm{GeV}/c^2$. Results with $\Delta s = 0$ and $M_A = 1.03\ \mathrm{GeV}/c^2$ are also shown. The data are from MiniBooNE [1].

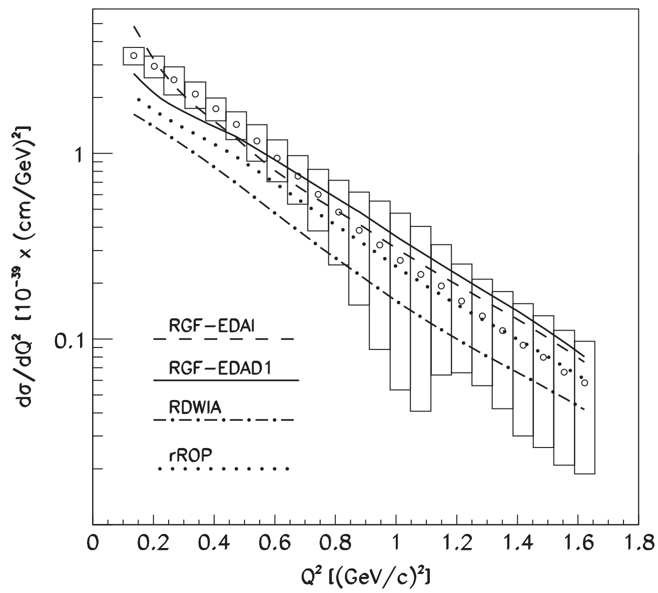

FIG. 3. NCE flux-averaged ($\nu N \rightarrow \nu N$) cross section as a function of Q^2, calculated with the RGF-EDAD1 (solid line) and RGF-EDAI (dashed line). The dotted and dotted-dashed lines are rROP and RDWIA results, calculated with the EDAI potential, respectively. The data are from MiniBooNE [1].

also shown again for a comparison. The MiniBooNE NCE cross section is nearly independent of Δs, as the combined effects on proton and neutron events almost cancel. In the calculations, a negative Δs produces an enhancement of the proton and a suppression of the neutron contribution, which are approximately of the same size (see also Ref. [23]). In the case of positive Δs, the effect is reversed. As a consequence, the effects of different values of Δs are minimal and smaller than the uncertainties due to M_A, whose value has a visible impact on the MiniBooNE NCE cross section.

In Fig. 3, we show our RGF results calculated with both EDAI and EDAD1 potentials and compare them with the RDWIA and the rROP results calculated with the EDAI potential. All these calculations have been performed with $M_A = 1.03\ \mathrm{GeV}/c^2$ and $\Delta s = 0$. The RGF cross sections with both optical potentials are larger than the RDWIA and the rROP ones. The rROP result, where a purely real optical potential is used, underestimates the experimental cross section for $Q^2 \leq 0.6\ (\mathrm{GeV}/c)^2$. We observe that a rROP calculation with a larger axial mass, e.g., $M_A \approx 1.3$–$1.4\ \mathrm{GeV}/c^2$, is able to reproduce the data with good accuracy. However, we note that, independently of its result in comparison with data, the rROP model, which is based on an energy-dependent potential, has important physical drawbacks. The RDWIA cross section with the EDAI potential is the same as already presented in Fig. 1 and gives in Fig. 3 the lowest cross section. The differences between the RGF results calculated with the two optical potentials are clearly visible, although not too large, the RGF-EDAI cross section being in good agreement with the shape and the magnitude of the experimental cross section, and the RGF-EDAD1 below the data only at the smallest values of Q^2 considered in the figure. The differences between the RGF results obtained with the two phenomenological optical potentials can give an idea of how uncertainties in the determination of this important ingredient can affect the predictions of the model. These differences are basically due to the different values of the imaginary parts of the two potentials, particularly for the energies considered in kinematics with the lowest values of Q^2. The real terms of the optical potentials are very similar for different parameterizations and give very similar results. In the rROP calculation shown in the figure, the real part of the EDAI potential has been used, but a calculation with EDAD1 would give in practice the same result.

The results displayed in Fig. 3 emphasize the important role of FSI and, in particular, of the imaginary part of the relativistic optical potential, which plays a different role in the different approaches. In the rROP, the imaginary part is neglected. In the RDWIA, it gives an absorption that accounts for the flux lost in each channel towards other channels which are not included in the model. In the RGF, the imaginary part redistributes the flux in all the final-state channels: in each channel, it accounts for the flux lost towards other inelastic channels and recovered for the inclusive scattering, making use of the dispersion relations. The results obtained in the different models give an idea of the relevance of these contributions. The larger cross sections in the RGF arise from the translation to the inclusive strength of the overall effect of inelastic channels. We have already noticed, however, that while the RDWIA neglects the contributions of some channels that can be included in the semi-inclusive reaction where only the emitted nucleon is detected, the RGF is appropriate for the inclusive scattering where only the final lepton is detected, and can take into account also contributions that are not included in the semi-inclusive process. From this point of view, the RDWIA can represent a lower limit and the RGF an upper limit to the calculated NCE cross sections.

The MiniBooNE Collaboration reported results for the flux-averaged differential cross section both in the CCQE and in the NCE scattering. In Ref. [1], these results are used to extract the NCE/CCQE ratio as a function of Q^2. This ratio can be useful to compare the results of the two measurements. In Fig. 4, we show our results for the NCE/CCQE ratio. We note that both NCE and CCQE cross sections are per target nucleon, thus there are 14/6 times more target nucleons in the numerator than in the denominator [1]. The results of the RGF and RDWIA with the EDAI potential are similar and within the experimental errors. This is in accordance with the observation that ratios of cross sections do not depend on FSI effects. The RDWIA model, which gives much lower predictions for the cross sections than the RGF, can produce results for the ratio close to the RGF ones and in overall agreement with the data. A more significant effect is given by a larger M_A. When $M_A = 1.39\ \mathrm{GeV}/c^2$ the NCE/CCQE ratio is enhanced up to ≈ 20%. This means that the axial mass has a different role in the NC and in the charged-current scattering.

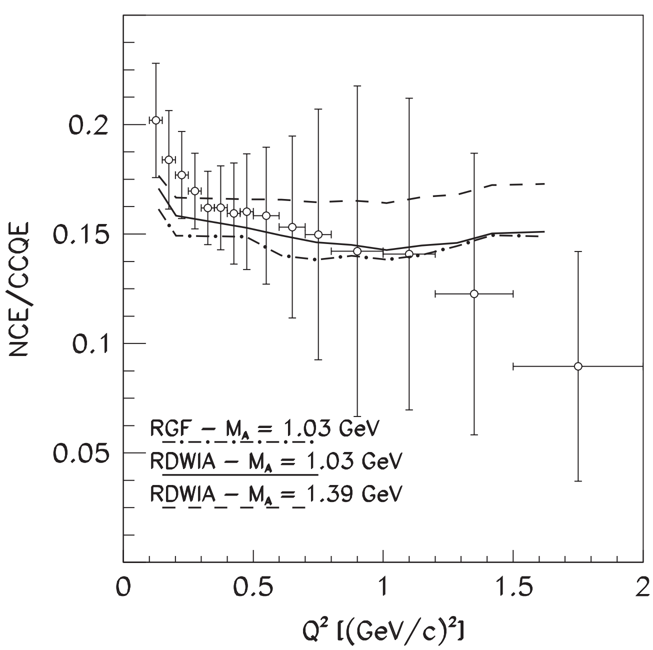

FIG. 4. The ratio of NCE/CCQE cross sections as a function of Q^2, calculated in the RDWIA with $M_A = 1.03$ (solid line) and $1.39\ \mathrm{GeV}/c^2$ (dashed line), and in the RGF with $1.03\ \mathrm{GeV}/c^2$ (dotted-dashed-line). The data are from MiniBooNE [1].

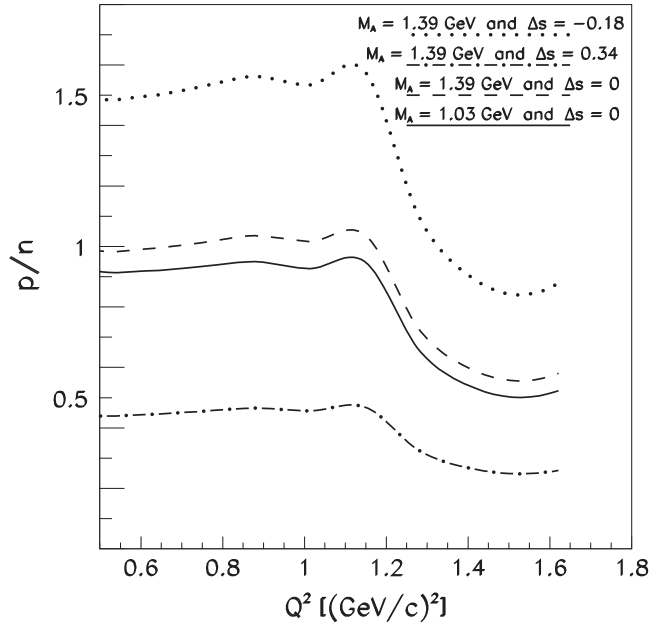

FIG. 5. The ratio of p/n cross sections as a function of Q^2, calculated in the RDWIA with three different values of Δs and $M_A = 1.39\ \mathrm{GeV}/c^2$. Results with $\Delta s = 0$ and $M_A = 1.03\ \mathrm{GeV}/c^2$ are also shown.

We have already noted that the MiniBooNE NCE cross section is nearly independent of Δs, as the combined effects on proton and neutron events almost cancel (see also Ref. [23]). In order to measure the strangeness contribution to the axial form factor the MiniBooNE Collaboration used the ratio of proton-to-nucleon cross sections for protons above the Cherenkov threshold as a function of the reconstructed nucleon kinetic energy [1]. In Fig. 5, we show our RDWIA results for the proton-to-neutron (p/n) ratio. This ratio was proposed as an efficient way to measure Δs [16,17] as the distortion effects should be largely reduced, but was later given up due to the difficulties associated with neutron detection. The p/n ratio is very sensitive to the strange-quark contribution, as the axial-vector strangeness Δs interferes with the isovector contribution to the axial form factor $g_A = 1.26$ with one sign in the numerator and with the opposite sign in the denominator. We already investigated in Ref. [19] the sensitivity of the p/n ratio to Δs as well as to the strange-quark contribution to the vector form factors. A large dependence on Δs was obtained, but also the effect of the magnetic strangeness was significant. However, we note that the p/n ratio of Fig. 5 is obtained by dividing the flux-integrated cross sections with one proton or one neutron in the final state and, moreover, that in the CH_2 target there are 8 protons and 6 neutrons. Thus, it is not straightforward to compare the results in Fig. 5 with those of Ref. [19]. Because of the independence of the p/n ratio on FSI, the results with the RGF and rROP models are similar to the RDWIA ones and are not shown in the figure.

The ratio is largely enhanced when a negative Δs is included and suppressed when a positive Δs is considered. When the axial mass is changed from the value obtained from the fit to the MiniBooNE NCE data ($M_A = 1.39\ \mathrm{GeV}/c^2$) to the measured world average value ($M_A = 1.03\ \mathrm{GeV}/c^2$), the p/n ratio is reduced up to $\approx 10\%$.

III. SUMMARY AND CONCLUSIONS

In this paper, we have compared the predictions of different relativistic descriptions of FSI for quasielastic NC neutrino-nucleus scattering with the MiniBooNE NCE data. In the RPWIA, FSI are simply neglected; in the rROP, they are described retaining only the real part of the relativistic energy-dependent optical potential; while in the RDWIA and in the RGF, the full complex optical potential, with its real and imaginary parts, is used to account for FSI.

The RDWIA is based on the same model that was widely and successfully applied to the analysis of the exclusive $(e, e'p)$ knockout reaction, where the final state is completely determined. In the exclusive reaction, the absorptive imaginary part of the optical potential, which accounts for the flux lost in the considered elastic channel to all inelastic final-state channels, gives a reduction of the calculated cross section that is required for a proper description of the experimental data. In the RDWIA, the cross section for the semi-inclusive reaction where only the emitted nucleon is detected is obtained from the sum of all the integrated exclusive one-nucleon knockout channels. In this case, however, the reduction produced in each channel by the imaginary part of the optical potential, which can be appropriate for the exclusive reaction, neglects some final-state channels which can contribute to the semi-inclusive reaction. All final-state channels are included in the RGF, where the flux lost in each channel is recovered in the other channels just by the imaginary part of the optical potential and the total flux is conserved. The RGF model is appropriate for the inclusive scattering, where only the outgoing lepton is detected, and with the use of the same complex optical potential, it provides a consistent treatment of FSI in the exclusive and in the inclusive process. In comparison with data, the RGF is able to give a good description of the (e, e') experimental cross sections in the QE region and also of the recent CCQE MiniBooNE data without the need to increase the standard value of the axial mass. The application of the RGF to the semi-inclusive NCE scattering can recover important contributions that are omitted in the RDWIA, and can give, from the comparison with the DWIA results, an indication of their relevance. It can also include, however, contributions of channels which are present only in the inclusive but not in the semi-inclusive reaction.

The RPWIA, rROP, and RDWIA results generally underpredict the MiniBooNE NCE data, the RDWIA giving the lowest cross section, unless the standard value of M_A is significantly enlarged. In contrast, the RGF results are in reasonable agreement with the experimental NCE cross section without the need to increase the standard value of M_A.

The enhancement of the RGF cross section can be ascribed to the contribution of reaction channels that are not included in the other models. It can be due, for instance, to rescattering processes of the nucleon in its way out of the nucleus, to non-nucleonic Δ excitations, which may arise during nucleon propagation, with or without real pion production, as well as to multinucleon processes. These contributions are not included explicitly in the model with a microscopic approach, but can be recovered, to some extent, in the RGF by the imaginary part of the phenomenological optical potential. With the use of such a phenomenological ingredient, however, we cannot disentangle the role of different reaction processes and explain in detail the origin of the recovered strength.

If all these contributions can be present in the inclusive scattering, the role of multinucleon processes in the NCE experimental data is not clear. It is a fact, however, that the theoretical analysis of MiniBooNE CCQE and NCE data presents a common problem: not only the simple RFG, but also other models, based on the IA and including only one-nucleon knockout contributions, require a larger value of M_A to reproduce the magnitude of the experimental cross sections. The calculations required for the theoretical analysis must consider the entire kinematical range of the relevant MiniBooNE neutrino energies. Additional complications may arise from the flux-average procedure to evaluate the CCQE and NCE cross sections, which implies a convolution of the double differential cross section over the neutrino spectrum. It has been argued [22,23] that, due to the uncertainties associated with the flux-average procedure, the MiniBooNE cross sections can include contributions from different kinematic regions, where other reaction mechanisms than one-nucleon knockout are known to be dominant. Moreover, further ambiguities arise for the MiniBooNE NCE cross section, which is given in bins where Q^2 is reconstructed from the kinetic energies of the ejected nucleons.

Models including other contributions than one-nucleon knockout, like our RGF, but also the model of Refs. [27–29], where multinucleon components are explicitly included, are able to describe both the MiniBooNE CCQE and NCE data without the need to change the value of the axial mass. The two models are different, but they seem to go in the same direction. In the RGF, however, the enhancement of the cross section cannot be attributed only to multinucleon processes, since we cannot disentangle the role of the various contributions included in the phenomenological optical potential.

In order to clarify the content of the enhancement of the RGF cross sections compared to those of the IA models, a careful evaluation of all nuclear effects and of the relevance of multinucleon emission and of some non-nucleonic contributions [61] is required. The comparison with the results of the RMF model, where only the purely nucleonic contribution is included, would be interesting for a deeper understanding. Processes involving two-body currents, whose importance has been discussed in Refs. [23,33,34,62], should also be taken into account explicitly and consistently in a model to clarify the role of multinucleon emission.

The RGF predictions are also affected by uncertainties in the determination of the phenomenological optical potential. At present, lacking a phenomenological optical potential which exactly fulfills the dispersion relations in the whole energy region of interest, the RGF prediction is not univocally determined from the elastic phenomenology. The differences between the RGF results obtained in the present investigation with the EDAI and EDAD1 potentials are visible, although smaller than for the CCQE cross sections in Ref. [52]. These differences are produced by the different imaginary part, which is the crucial ingredient in both RDWIA and RGF calculations, the real part being very similar for different parameterizations of the optical potential. It is interesting to notice that the best predictions in comparison with both CCQE and NCE data are given by the EDAI potential, which is also able to give the better description of the elastic proton-^{12}C phenomenology. A better determination of a phenomenological relativistic optical potential, which closely fulfills the dispersion relations, would be anyhow desirable and deserves further investigation.

In this work, we have investigated also the role of a possible strange-quark contribution Δs to the axial nucleon form factor. The calculated cross sections are almost unaffected by Δs, as the combined effects of Δs on proton and neutron events almost cancel. As a consequence, also the ratio of NCE/CCQE cross sections is unaffected by Δs if both proton and neutron events are included in the NCE cross section. Experimental information on the strange-quark contribution to the NCE/CCQE ratio can be obtained if only proton (or neutron) emission is considered. The p/n ratio is very sensitive to the strange-quark contribution, but requires the explicit separation of the proton and neutron cross sections.

ACKNOWLEDGMENTS

We are grateful to Franco Capuzzi for useful discussions. This work was partially supported by the Italian MIUR through the PRIN 2009 research project.

[1] A. A. Aguilar-Arevalo *et al.* (MiniBooNE Collaboration), Phys. Rev. D **82**, 092005 (2010).

[2] A. A. Aguilar-Arevalo *et al.* (MiniBooNE Collaboration), Phys. Rev. D **81**, 092005 (2010).

[3] Y. Nakajima *et al.* (SciBooNE Collaboration), Phys. Rev. D **83**, 012005 (2011).

[4] Q. Wu *et al.* (NOMAD Collaboration), Phys. Lett. B **660**, 19 (2008).

[5] V. Lyubushkin *et al.* (NOMAD Collaboration), Eur. Phys. J. C **63**, 355 (2009).

[6] P. Adamson *et al.* (MINOS Collaboration), Phys. Rev. D **81**, 072002 (2010).

[7] A. Acha *et al.* (HAPPEX Collaboration), Phys. Rev. Lett. **98**, 032301 (2007).

[8] D. Casper, Nucl. Phys. B, Proc. Suppl.**112**, 161 (2002).

[9] Y. Hayato, Nucl. Phys. B, Proc. Suppl. **112**, 171 (2002).

[10] R. Gran *et al.* (K2K Collaboration), Phys. Rev. D **74**, 052002 (2006).

[11] V. Bernard, L. Elouadrhiri, and U. G. Meissner, J. Phys. G **28**, R1 (2002).

[12] A. Bodek, S. Avvakumov, R. Bradford, and H. Budd, Eur. Phys. J. C **53**, 349 (2008).

[13] L. A. Ahrens *et al.*, Phys. Rev. D **35**, 785 (1987).

[14] G. T. Garvey, W. C. Louis, and D. H. White, Phys. Rev. C **48**, 761 (1993).

[15] S. F. Pate, Phys. Rev. Lett. **92**, 082002 (2004).

[16] G. Garvey, E. Kolbe, K. Langanke, and S. Krewald, Phys. Rev. C **48**, 1919 (1993).

[17] W. M. Alberico, S. M. Bilenky, and C. Maieron, Phys. Rep. **358**, 227 (2002).

[18] A. Meucci, C. Giusti, and F. D. Pacati, Nucl. Phys. **A744**, 307 (2004).

[19] A. Meucci, C. Giusti, and F. D. Pacati, Nucl. Phys. **A773**, 250 (2006).

[20] S. Boffi, C. Giusti, and F. D. Pacati, Phys. Rep. **226**, 1 (1993).

[21] S. Boffi, C. Giusti, F. D. Pacati, and M. Radici, *Electromagnetic Response of Atomic Nuclei*, Oxford Studies in Nuclear Physics Vol. 20 (Clarendon Press, Oxford, 1996).

[22] O. Benhar, P. Coletti, and D. Meloni, Phys. Rev. Lett. **105**, 132301 (2010).

[23] O. Benhar and G. Veneziano, Phys. Lett. B **702**, 433 (2011).

[24] A. V. Butkevich, Phys. Rev. C **82**, 055501 (2010).

[25] C. Juszczak, J. T. Sobczyk, and J. Zmuda, Phys. Rev. C **82**, 045502 (2010).

[26] A. V. Butkevich and D. Perevalov, Phys. Rev. C **84**, 015501 (2011).

[27] M. Martini, M. Ericson, G. Chanfray, and J. Marteau, Phys. Rev. C **80**, 065501 (2009).

[28] M. Martini, M. Ericson, G. Chanfray, and J. Marteau, Phys. Rev. C **81**, 045502 (2010).

[29] M. Martini, M. Ericson, and G. Chanfray, Phys. Rev. C **84**, 055502 (2011).
[30] J. Nieves, I. Ruiz Simo, and M. J. Vicente Vacas, Phys. Rev. C **83**, 045501 (2011).
[31] J. Nieves, I. Ruiz Simo, and M. J. Vicente Vacas, arXiv:1106.5374.
[32] A. De Pace, M. Nardi, W. M. Alberico, T. W. Donnelly, and A. Molinari, Nucl. Phys. **A726**, 303 (2003).
[33] J. E. Amaro, M. B. Barbaro, J. A. Caballero, T. W. Donnelly, and C. F. Williamson, Phys. Lett. B **696**, 151 (2011).
[34] J. E. Amaro, M. B. Barbaro, J. A. Caballero, T. W. Donnelly, and J. M. Udías, Phys. Rev. D **84**, 033004 (2011).
[35] J. M. Udías, P. Sarriguren, E. Moya de Guerra, E. Garrido, and J. A. Caballero, Phys. Rev. C **48**, 2731 (1993).
[36] J. M. Udías, P. Sarriguren, E. Moya de Guerra, E. Garrido, and J. A. Caballero, Phys. Rev. C **51**, 3246 (1995).
[37] A. Meucci, C. Giusti, and F. D. Pacati, Phys. Rev. C **64**, 014604 (2001).
[38] A. Meucci, Phys. Rev. C **65**, 044601 (2002).
[39] M. Radici, A. Meucci, and W. H. Dickhoff, Eur. Phys. J. A **17**, 65 (2003).
[40] T. Tamae, Y. Sato, T. Yokokawa, Y. Asano, M. Kawabata, O. Konno, I. Nakagawa, I. Nishikawa, K. Hirota, H. Yamazaki, R. Kimura, H. Miyase, H. Tsubota, C. Giusti, and A. Meucci, Phys. Rev. C **80**, 064601 (2009).
[41] C. Giusti, A. Meucci, F. D. Pacati, G. Co', and V. De Donno, Phys. Rev. C **84**, 024615 (2011).
[42] C. Maieron, M. C. Martinez, J. A. Caballero, and J. M. Udías, Phys. Rev. C **68**, 048501 (2003).
[43] J. A. Caballero, Phys. Rev. C **74**, 015502 (2006).
[44] J. A. Caballero, M. C. Martinez, J. L. Herraiz, and J. M. Udías, Phys. Lett. B **688**, 250 (2010).
[45] A. Meucci, C. Giusti, and F. D. Pacati, Nucl. Phys. **A739**, 277 (2004).
[46] A. Meucci, F. Capuzzi, C. Giusti, and F. D. Pacati, Phys. Rev. C **67**, 054601 (2003).
[47] A. Meucci, J. A. Caballero, C. Giusti, F. D. Pacati, and J. M. Udías, Phys. Rev. C **80**, 024605 (2009).
[48] A. Meucci, J. A. Caballero, C. Giusti, and J. M. Udías, Phys. Rev. C **83**, 064614 (2011).
[49] Y. Horikawa, F. Lenz, and N. C. Mukhopadhyay, Phys. Rev. C **22**, 1680 (1980).
[50] F. Capuzzi, C. Giusti, and F. D. Pacati, Nucl. Phys. **A524**, 681 (1991).
[51] F. Capuzzi, C. Giusti, F. D. Pacati, and D. N. Kadrev, Ann. Phys. (N.Y.) **317**, 492 (2005).
[52] A. Meucci, M. B. Barbaro, J. A. Caballero, C. Giusti, and J. M. Udías, Phys. Rev. Lett. **107**, 172501 (2011).
[53] A. Meucci, C. Giusti, and F. D. Pacati, Phys. Rev. C **77**, 034606 (2008).
[54] A. Meucci, C. Giusti, and F. D. Pacati, Acta Phys. Pol. B **37**, 2279 (2006).
[55] C. Giusti, A. Meucci, and F. D. Pacati, Acta Phys. Pol. B **40**, 2579 (2009).
[56] B. D. Serot and J. D. Walecka, Adv. Nucl. Phys. **16**, 1 (1986).
[57] M. M. Sharma, M. A. Nagarajan, and P. Ring, Phys. Lett. B **312**, 377 (1993).
[58] G. A. Lalazissis, J. König, and P. Ring, Phys. Rev. C **55**, 540 (1997).
[59] B. C. Clark, in *Proceedings of the Workshop on Relativistic Dynamics and Quark-Nuclear Physics*, edited by M. B. Johnson and A. Picklesimer (Wiley, New York, 1986), p. 302.
[60] E. D. Cooper, S. Hama, B. C. Clark, and R. L. Mercer, Phys. Rev. C **47**, 297 (1993).
[61] T. Leitner and U. Mosel, Phys. Rev. C **81**, 064614 (2010).
[62] A. Bodek, H. Budd, and M. Christy, Eur. Phys. J. C **71**, 1726 (2011).